

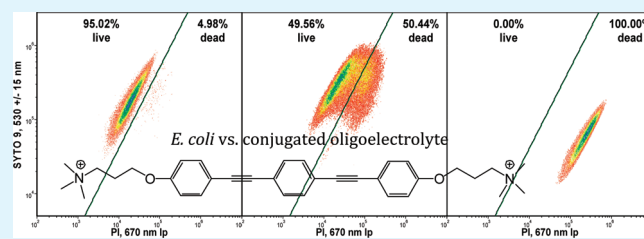
# Rapid Evaluation of the Antibacterial Activity of Arylene–Ethynylene Compounds

Thomas S. Corbitt, Zhijun Zhou, Yanli Tang, Steven W. Graves, and David G. Whitten\*

Center for Biomedical Engineering, Department of Chemical & Nuclear Engineering, University of New Mexico, Albuquerque, New Mexico 87131, United States

**ABSTRACT:** A series of oligo(arylene–ethynylene) (1–3 repeat units) compounds functionalized with quaternary ammonium groups was screened for their antibacterial activity in the dark and with activation by long-wavelength (365 nm) UV irradiation. Several of these compounds have effective bactericidal activity (>99.9% killing) at concentrations between 0.01 and 10  $\mu\text{g}/\text{mL}$ . Our approach uses flow cytometry to rapidly screen and evaluate the susceptibility of bacterial populations. The rapidity, high information content, and accuracy of this approach make it an extremely valuable method for the study of antibacterial compounds.

**KEYWORDS:** flow cytometry, antimicrobial activity, oligo(arylene ethynylene)s, conjugated electrolytes, light-activated biocide, photodynamic therapy



## INTRODUCTION

Chemical agents that can selectively inactivate or destroy biological threats while having a low toxicity toward humans and the environment are desirable for obvious reasons. A number of cationic polyelectrolytes (CPEs) have been found to be effective bactericides.<sup>1–7</sup> Many of these compounds are water-soluble and exhibit an affinity for bacterial cell membranes, causing membrane disruption, agglomeration, and bacterial death. Our particular focus is on a family of conjugated oligomers synthesized in our laboratories that was previously shown to have antimicrobial properties.<sup>8–11</sup> These compounds have structures based on arylene–ethynylene repeat units that are functionalized by one of several types of tetraalkylammonium side groups. These compounds show remarkable bactericidal activity, and layer-by-layer constructs made using alternating anionic and cationic polymers of this family have significant bacterial sequestration properties in solution and on fibers and surfaces.<sup>11</sup> Model membrane studies also indicate that these compounds have a high affinity for bacterial membranes but a low affinity for mammalian membranes.<sup>12</sup> A number of the compounds have been physisorbed or chemically grafted onto cotton and silk fabrics and silica surfaces while retaining their fluorescent and biocidal properties.<sup>13</sup> The synthesis and characterization of these compounds has complemented other efforts within the group that seek to correlate the biocidal activity with the photophysical properties of the CPEs and with the characteristics of target bacterial membranes.<sup>14–18</sup>

While a number of the compounds are active in the dark, their biocidal effects are, in most cases, strongly enhanced by photoexcitation in the near-UV ( $\sim 365 \text{ nm}$ ) for the shorter oligomers and in the visible ( $400$ – $450 \text{ nm}$ ) for the higher-repeat-unit (7–50) polymers. Efficient light-induced interfacial generation of singlet oxygen is occurring in these systems and has been

quantified;<sup>18,19</sup> this is believed to contribute considerably to their activity in light. Several of the complexes are quite effective against a variety of bacteria, both Gram positive [*Bacillus atrophaeus* (both vegetative cells and spores), *Staphylococcus aureus*, and *Staphylococcus epidermidis*] and Gram negative (*Pseudomonas aeruginosa*, *Escherichia coli*, and *Cobetia marina*). The work presented here encompasses studies using *S. aureus*, *S. epidermidis*, and *E. coli*, for which the light-induced killing has been observed to be as high as 7 log in some cases (*E. coli* and *S. epidermidis*, 30 min light exposure), with some of the oligomers also showing substantial lethality at similar times in the dark at higher concentrations ( $>10 \mu\text{g}/\text{mL}$ ). Two oligomers synthesized in our laboratory and screened against target bacteria are shown in Scheme 1. The synthetic methods are described elsewhere.<sup>16–18</sup>

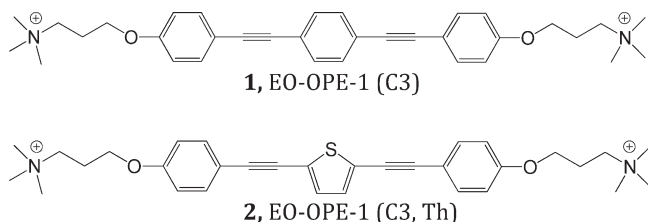
Flow cytometry involves the generation of a particle stream by various means, usually in a liquid, which then undergoes sequential optical analysis. With this technique, analysis of the microorganisms can potentially be carried out at a number of levels, from simple detection or identification to counting to characterization of the viability, growth, metabolism, and interaction with various chemical and physical agents. Since the early 1980s, a number of researchers have been able to use this technique to differentiate bacterial populations using various fluorescent labels and probes.<sup>20–23</sup> With the appropriate choice of stains, staining protocols, and gating, this approach has been refined to provide results that correlate well with plating and optical density approaches.<sup>24–27</sup> Scatter parameters from flow cytometry coupled with simultaneous confocal microscopy imaging also provide

**Received:** March 4, 2011

**Accepted:** June 29, 2011

**Published:** June 29, 2011

**Scheme 1. Structures of Two Functionalized CPE Complexes**



insight into potential morphological changes that occur upon bacterial injury.

In our studies, flow cytometry paired with confocal laser scanning microscopy (CLSM) and single- and multiple-staining methods has been used to rapidly screen the CPEs for biocidal activity. The flow cytometry technique provides the quantitative determination of the chemically induced killing, natural attrition rates, staining efficiencies, and autofluorescence of bacteria, while CLSM is used to corroborate the staining and can visually indicate morphological changes and degree of aggregation of the bacteria after exposure to the compounds of interest in dark and light-exposed conditions.

## ■ EXPERIMENTAL METHODS

All bacterial work was carried out under sterile conditions (flaming, alcohol rinse, etc.). Bacteria for testing, *E. coli* (ATCC 29425), *S. epidermidis* (ATCC 35984), and *S. aureus* (ATCC 25923), were initially obtained from ATCC and used to generate a stock culture stored in 20% glycerol at  $-70^{\circ}\text{C}$ . The thawed stock culture was used to inoculate an agar slant, which was then stored at  $4^{\circ}\text{C}$  for up to 2 weeks. Colonies from the slant were used to inoculate flasks (250 mL, with 50 mL broth) to grow cultures in Nutrient Broth (Difco). This flask was then sealed with a foam stopper covered by aluminum foil, in a shaker/incubator held at  $30^{\circ}\text{C}$  for 18 h.

The overnight bacteria destined for direct experimentation were prepared by centrifugation at  $4^{\circ}\text{C}$  at 10K rpm for 30 min in an Eppendorf 5415C centrifuge, and the supernatant was removed and discarded. The remaining pellet was resuspended in 40 mL of a 0.85% NaCl solution and recentrifuged under the same conditions. This cycle was repeated for a total of three washes, and counting was carried out in a hemocytometer in order to normalize bacterial concentrations. The bacteria were used immediately after their preparation to preserve live population.

*E. coli*, *S. epidermidis*, and *S. aureus* overnight batch cultures with populations of  $\sim 2 \times 10^9$  bacteria  $\text{mL}^{-1}$  were diluted to between  $10^6$  and  $10^7$   $\text{mL}^{-1}$  in a 0.85% NaCl buffer for flow samples. The sample set typically contained live and dead controls, split into multiple aliquots for varied staining procedures. For example, unstained, propidium iodide (PI)-only stained and doubly stained (PI and the appropriate permeant SYTO dye) controls were used to determine the autofluorescence of the vegetative cells. Biocidal candidate compounds were added to these samples at multiple concentrations between 0.001 and 10  $\mu\text{g mL}^{-1}$ . SYTO 9, SYTO 24, and PI stains were used in the flow cytometer experiments, with a 15 min minimum incubation period. Light exposures were between 30 and 120 min in an enclosed photochamber (LuzChem ORG) with near-UV (365 nm) excitation sources. This device has a sample capacity of 16 microcentrifuge tubes or cuvettes and also has a rotating carousel that provides for uniform exposures of around 9  $\text{mW cm}^{-2}$ .

**Table 1. Fluorescence Detection Parameters in the Accuri C6 Flow Cytometer**

filter	excitation source (nm)	detection range (nm)
FL1	488	$530 \pm 15$
FL2	488	$585 \pm 20$
FL3	488	670 long pass
FL4	640	$675 \pm 12.5$

Flow cytometric studies herein were done using an Accuri C6 flow cytometer, a compact unit with four fluorescence and two scatter detectors. This instrument is capable of processing up to 10 000 events  $\text{s}^{-1}$  and sample concentrations near  $10^7$  cells  $\text{mL}^{-1}$ . The C6 uses peristaltic pumps for transport, allowing for cell concentration determination by precisely metering the volume. The instrument has two lasers and four fluorescence detectors, set up with the optical filters shown in Table 1. Data are collected on forward scatter (FSC) and side scatter (SSC) (from the 488 nm laser) and all four fluorescence channels in every run. The Accuri C6 was calibrated with eight peak rainbow beads (Spherotech, Inc.) and proved to be quite stable over time in fluorescence as gauged by coefficient of variation (CV) values. The instrument was backflushed between sample types in order to minimize residual contamination. The system was also cleaned and decontaminated after each use to eliminate any stains or bacterial debris that might bind to the flow cytometer tubing.

For the selected stains, the most useful representation for gating the data was the bivariate plot of FL1 ( $530 \pm 15$  nm—"green"—live) for the SYTO 9 and SYTO 24 permeant stains and FL3 (670 nm long pass—"red"—dead) for the PI. For the flow cytometric bivariate plot graphics in this paper, we have followed the convention of having the green fluorescence channel (FL1) on the Y axis and the red fluorescence channel (FL3) on the X axis. The virtual "life cycle" could be followed through the progression of events moving roughly clockwise on these plots, starting in the lower left with unstained live controls, moving upward once stained, and then transitioning to the right with an increase in the membrane permeability and finally downward with a further loss of the membrane integrity. The last three stages of this process are shown in Figure 1.

For corroborative evidence, comparison plating on TSB agar plates was done on selected samples split from the corresponding samples used for flow cytometry testing. These were incubated overnight (18 h) at  $30^{\circ}\text{C}$ .

In any given experimental set, consistent scattering thresholds were applied across all samples and 10K–50K events were collected per run. For the compounds showing high activity, runs of up to 10 000 000 events were carried out to firmly establish the log killing values. The working scattering thresholds that we have established are (FSC-H) as follows: *S. aureus*, 40 000–60 000; *E. coli*, 15 000–30 000. These values are dependent on the growth phase and media, making it especially important to have consistent growth conditions. Both of these scattering thresholds were complemented by a secondary fluorescence threshold between 100 and 1000 (typically  $\sim 250$ ) in FL1 or FL3. Because of the pronounced spreading in the scatter, gate settings were usually adjusted to include at least 75% of the total events and were centered on mean values of the signals for both FSC and SSC. These settings were then optimized by monitoring CV values for the fluorescent channels of interest (FL1 and FL3). The experimental data were analyzed using the CFlow software available on the Accuri C6 and with FCS Express 3.0 from DeNovo Software.

## ■ RESULTS AND DISCUSSION

The effects of the CPEs on the bacteria in most every case were quite pronounced, as observed by flow cytometry. FSC is generally

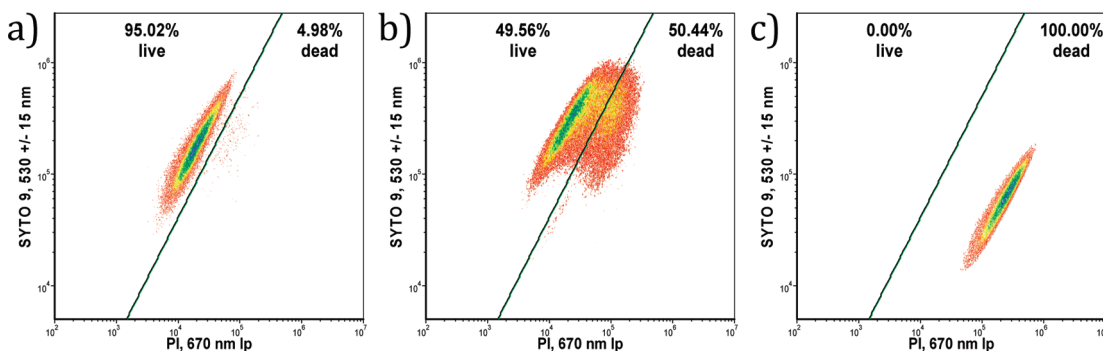


Figure 1. Doubly stained sample of *E. coli*: (a) live control; (b) after exposure to compound 1 in the dark; (c) after light exposure with compound 1.

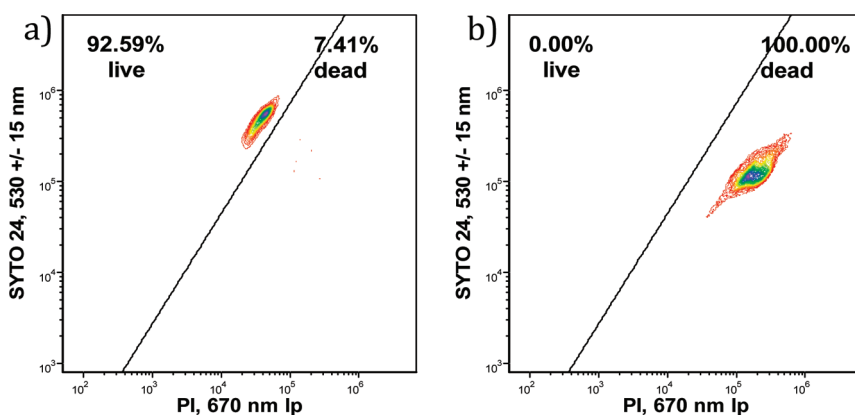


Figure 2. *S. aureus* (a) live control (dark, 60 min) and (b) dead control (heat-killed at 90 °C for 2.5 h).

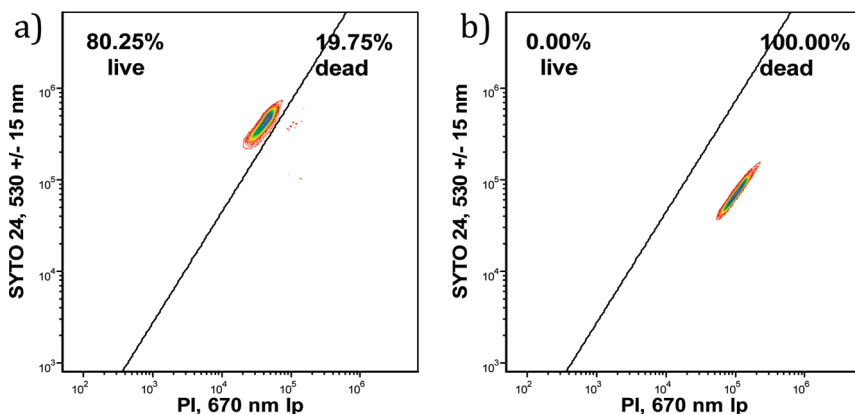


Figure 3. *S. aureus* exposed to 1  $\mu$ g/mL of 2 for 60 min (a) in the dark and (b) with light exposure.

correlated to the particle size, while SSC is more closely related to the surface complexity characteristics of the particle; for bacteria, this is likely indicative of the membrane roughness.<sup>28</sup> In our screening runs, the signals for FSC and SSC tended to spread significantly, sometimes with one clearly affected more than the other. This spreading is most likely due to two factors: (1) the agglomeration of bacteria that was observed by CLSM in this and many prior experiments and (2) the variability in the uptake of the stains among individual bacteria, clusters, and debris particles (which may also be contained in the agglomerates). This contributed to a broadening in the distribution and an increase

in the range of intensities of both scatter and fluorescence, although this was likely mitigated somewhat by the narrowing of the orifice ( $\sim 40 \mu\text{m}$  maximum particle size<sup>29</sup>) through which any clustered material had to pass. This same reasoning would suggest that many agglomerated bacteria were possibly not counted because of the fact that the instrument rejects the acquisition of data if a pulse width exceeds a preset limit. Also, for cells that were damaged and permeabilized to the PI stain, the increase in the range of SSC was less pronounced, possibly because of the refractive index differential between the cells and the solution being diminished by equilibrium processes.

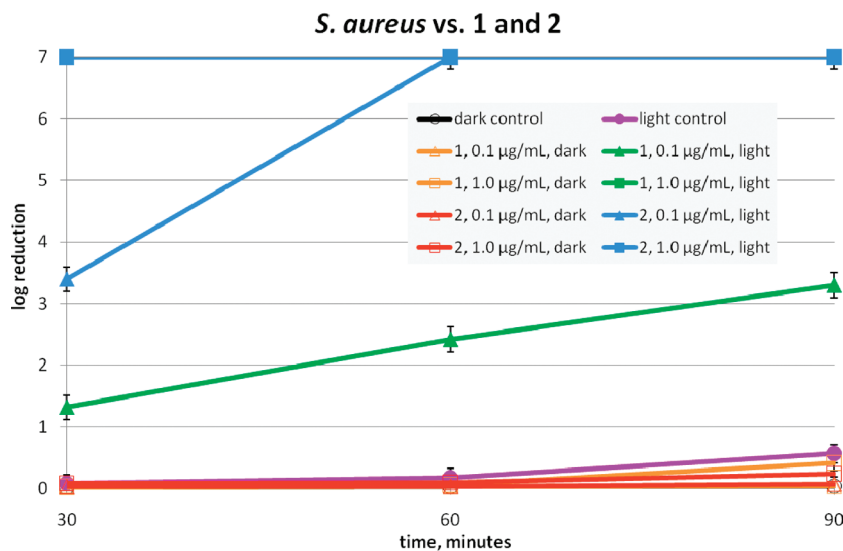


Figure 4. Log killing of *S. aureus* over time by **1** and **2** in both dark and light-exposed conditions at two concentrations (0.1 and 1.0 µg/mL).

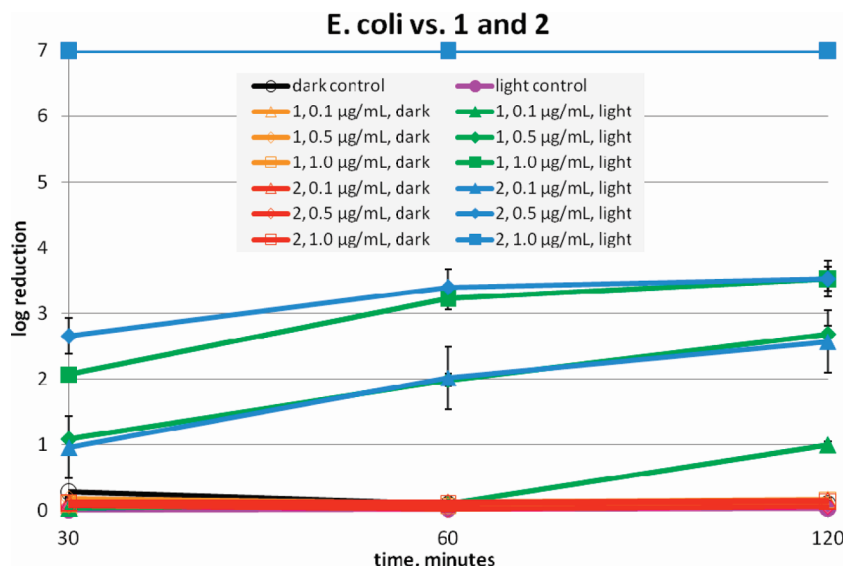


Figure 5. Biocidal effect of **1** [EO-OPE1-(C3)] and **2** [EO-OPE1-(C3,Th)] on *E. coli* in the dark and light at three different concentrations (0.1, 0.5, and 1.0 µg/mL) and at three times (30, 60, and 120 min).

At concentrations down to 0.01 µg/mL, the light-activated effects of the oligomers were unambiguous, as can be seen in Figures 3 and 6. Here the PI staining is quantitative in the light-exposed sample, and the corresponding red fluorescence has increased by an order of magnitude over the live control. This indicates that **2** with light exposure is extremely effective in permeabilizing the bacterial membrane of Gram positive bacteria.

The choices of which channel and where to set the lower boundary (threshold) for the signal intensity are also critical ones. Since the particles of interest (bacteria) are near the lower size limits for the instrument, a triggering threshold of less than 80 000 in FSC was usually required for achieving reasonable scatter populations. This threshold was combined with small-valued fluorescence cutoffs (100–1000) in order to improve CV values and minimize triggering from cellular debris. Values higher than 1000 would typically begin to eliminate legitimate data. The

numbers of events per microliter registered by the flow cytometer were then compared to the cell count from a hemocytometer for consistency and, insofar as practical, parameters were adjusted to match the counts. Care should be taken in assigning these multiple flow cytometric parameters, balancing the need for careful population identification and for the setting of thresholds and gating to optimize the capture of data from those populations.

The fluorescence signal strength can shift between samples with different compounds and with differing concentrations; therefore, the gating must sometimes be adjusted between sample types to fit the new medians of population. Usually, this is not a large shift and the population profiles or contour shapes tend to remain the same, so setting the new gates only requires the adjustment of existing gates along one axis. However, in samples treated with oligomers **1** and **2**, the bacteria appear heavily damaged, even with low exposure times at concentrations

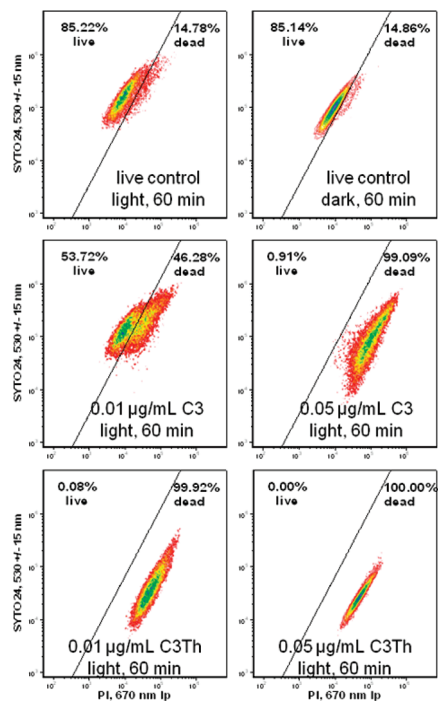


**Figure 6.** Effects of **1** (“C3”) and **2** (“C3Th”) on *S. epidermidis* at lower concentrations.

of  $<0.1 \mu\text{g/mL}$ . Here, we must assume that the membrane integrity is highly impacted, causing rapid leakage and/or quenching of the SYTO permeant stain during equilibration with the suspension medium. This is reflected in the significant movement of the population by an order of magnitude lower in FL1 and about the same amount higher in FL3 (downward and to the right in the bivariate plot) as compared to samples with less active compounds.

The demarcation line of the bacteria as “live” and “dead” is based on population geometric means established by untreated live (as in Figures 1a, 2a, and 3a) and dead [Figure 1c (with compound **1**), heat-killed, Figure 2b] control samples. Plate counting resulted in no viable colonies for samples showing  $>95\%$  killing by flow cytometry. This indicates that the flow cytometry numbers are probably rather conservative for evaluating the antimicrobial activity in this system.

The flow cytometry data in Figures 4 and 5 gathered on the oligomeric compounds **1** and **2** show that they are effective biocides primarily under light conditions. The greatest impact was observed with **2**, which proved to be 100% lethal ( $>6$  log killing, 0 live bacteria out of 1 000 000 counts) to *S. aureus* after 30 min of light exposure at a concentration of  $0.1 \mu\text{g/mL}$ . CV values for these experiments ranged from 7 to 30% and averaged about 12%, quite reasonable for biological samples of this type.

Evaluation of the control samples that had undergone light exposure was also important with the oligomers because these molecules require shorter wavelength excitation for activation. This affected *S. aureus* more than *E. coli*, and in some instances the attrition of the bacteria was significant (see Figure 4, light control). For *E. coli* at the longest light exposure time (120 min), the maximum amount of cell attrition for any of the live controls was measured at 22%. Given this caveat, the significant differences between the experimental samples and controls can still be observed.

The effects of **1** and **2** on *S. epidermidis* at lower concentrations ( $0.01$  and  $0.05 \mu\text{g/mL}$ ) can be seen in Figure 6. Studies are underway now to bracket the lower active concentrations for a number of these compounds, and the thiophenyl-substituted compound in particular still shows appreciable biocidal activity against *S. epidermidis* (1–3 log reduction) at concentrations of  $0.001 \text{ mg/mL}$ .

## CONCLUSIONS

A number of arylene–ethynylene compounds have undergone preliminary screening with flow cytometry, confirming the observations of antimicrobial effects on bacterial cells made in earlier experiments with confocal microscopy. Some of the oligomers seem especially potent and are seen to cause quantitative or near-quantitative permeabilization of the bacteria.

Because different antibacterial agents may have different direct and indirect impacts on various functions in different bacteria, it is obviously important to be able to track more than one parameter to understand the effects of the CPEs on the bacteria. The multiple parameters available in flow cytometry do help to accurately discriminate certain properties, but these properties may be difficult to uncouple from each other because of factors such as variation in the bacterial sizes, orientation of asymmetric microbes in the flow stream, and, perhaps most importantly, variations in staining. Some early attempts to correlate plate counting for bacterial susceptibility with flow cytometric evaluations differed by more than a factor of 5.<sup>30</sup> However, more recent studies have demonstrated that flow cytometry can produce comparable and consistent results, which can be very sensitive to bacterial metabolic states while simultaneously providing insight into size and surface morphology changes.<sup>31–33</sup> Once the intrinsic properties of bacterial cells are sufficiently characterized, flow cytometry, with or without a given set of stains, yields much useful information.<sup>30,34</sup> These observations can shed light on both the direct and indirect impact of antimicrobials on microorganisms and enable the identification of mechanisms involved in bacterial death.<sup>35–40</sup> Given its rapid analysis times, low volume requirements, high sensitivity, and synchronous measurement of fluorescence sensitivity, flow cytometry can be a powerful tool for the evaluation of bacterial susceptibility and can aid in the discovery of new antimicrobial agents.

Sample processing in flow cytometry usually only takes a couple of minutes per sample, much faster than either plate counting (overnight) or CLSM. With flow cytometry, measurement of the particle characteristics can be very precise, but selection of the gating parameters, triggering thresholds, sample concentrations, staining protocols, and flow rates must be optimized. Because most bacteria, including those studied herein, are at the lower end of the size range for the instrument, noise from the background (stray light and diffraction from fluid density variations) require thresholds that necessarily eliminate some real events. On the bright side, photobleaching is less of a problem when using a flow cytometer because each cell is exposed to excitation light for just a few microseconds as it passes through the beam, giving much more flexibility in the choice of stains. In all cases, the relationship between staining conditions and viability must be judged carefully.

This family of oligomeric materials shows great promise in rapidly reducing populations of pathogens. The low antagonism toward mammalian cells indicates that these materials could potentially be employed in general use biocidal applications.

We have also covalently grafted other compounds of this type to silicon microspheres and fiber surfaces and envision their potential incorporation into bandages, clothing, filters, and medical devices such as catheters and endoscopic tools. With their greatly increased activity under compatible irradiation, this series of compounds may also benefit patients through application in photodynamic therapy.

## ■ AUTHOR INFORMATION

### Corresponding Author

\*E-mail: whitten@langmuir.acs.org.

## ■ ACKNOWLEDGMENT

We gratefully acknowledge the DTRA (Contract W911NF-07-1-0079) for funding this work and Dr. Dimitri Dascier for assistance in plating.

## ■ REFERENCES

- (1) Arnt, L.; Tew, G. N. *Langmuir* **2003**, *19* (6), 2404–2408.
- (2) Ishitsuka, Y.; Arnt, L.; Ratajczak, M.; Majewski, J.; Tew, G.; Kjaer, K.; Lee, K. Y. C. *Biophys. J.* **2005**, *88* (1), 421A–421A.
- (3) Codling, C. E.; Maillard, J. Y.; Russell, A. D. *J. Antimicrob. Chemother.* **2003**, *51* (5), 1153–1158.
- (4) Kenawy, E. R.; Abdel-Hay, F. I.; Shahada, L.; El-Shanshoury, A.; El-Newehy, M. H. *J. Appl. Polym. Sci.* **2006**, *102* (5), 4780–4790.
- (5) Lin, J.; Qiu, S.; Lewis, K.; Klibanov, A. M. *Biotechnol. Prog.* **2002**, *18* (5), 1082–1086.
- (6) Siddiqui, A.; Schultz, A. K. Antimicrobial polymer latexes derived from unsaturated quaternary ammonium compounds and antimicrobial coatings, sealants, adhesives and elastomers produced from such latexes. U.S. Patent 6,492,445, Dec 10, 2002.
- (7) Thorsteinsson, T.; Masson, M.; Kristinsson, K. G.; Hjalmarsdottir, M. A.; Hilmarsdottir, H.; Loftsson, T. *J. Med. Chem.* **2003**, *46* (19), 4173–4181.
- (8) Lu, L. D.; Rininsland, F. H.; Wittenburg, S. K.; Achyuthan, K. E.; McBranch, D. W.; Whitten, D. G. *Langmuir* **2005**, *21* (22), 10154–10159.
- (9) Chemburu, S.; Corbitt, T. S.; Ista, L. K.; Ji, E.; Fulghum, J.; Lopez, G. P.; Ogawa, K.; Schanze, K. S.; Whitten, D. G. *Langmuir* **2008**, *24* (19), 11053–11062.
- (10) Corbitt, T. S.; Ding, L. P.; Ji, E. Y.; Ista, L. K.; Ogawa, K.; Lopez, G. P.; Schanze, K. S.; Whitten, D. G. *Photochem. Photobiol. Sci.* **2009**, *8* (7), 998–1005.
- (11) Corbitt, T. S.; Sommer, J. R.; Chemburu, S.; Ogawa, K.; Ista, L. K.; Lopez, G. P.; Whitten, D. G.; Schanze, K. S. *ACS Appl. Mater. Interfaces* **2009**, *1* (1), 48–52.
- (12) Wang, Y.; Tang, Y.; Zhou, Z.; Ji, E.; Lopez, G. P.; Chi, E. Y.; Schanze, K. S.; Whitten, D. G. *Langmuir* **2010**, *26* (15), 12509–12514.
- (13) Ogawa, K.; Chemburu, S.; Lopez, G. P.; Whitten, D. G.; Schanze, K. S. *Langmuir* **2007**, *23* (8), 4541–4548.
- (14) Ding, L. P.; Chi, E. Y.; Chemburu, S.; Ji, E.; Schanze, K. S.; Lopez, G. P.; Whitten, D. G. *Langmuir* **2009**, *25* (24), 13742–13751.
- (15) Wang, Y.; Tang, Y. L.; Zhou, Z. J.; Ji, E.; Lopez, G. P.; Chi, E. Y.; Schanze, K. S.; Whitten, D. G. *Langmuir* **2010**, *26* (15), 12509–12514.
- (16) Tang, Y. L.; Zhou, Z. J.; Ogawa, K.; Lopez, G. P.; Schanze, K. S.; Whitten, D. G. *Langmuir* **2009**, *25* (1), 21–25.
- (17) Tang, Y. L.; Zhou, Z. J.; Ogawa, K.; Lopez, G. P.; Schanze, K. S.; Whitten, D. G. *J. Photochem. Photobiol. A* **2009**, *207* (1), 4–6.
- (18) Zhou, Z. J.; Corbitt, T. S.; Parthasarathy, A.; Tang, Y. L.; Ista, L. F.; Schanze, K. S.; Whitten, D. G. *J. Phys. Chem. Lett.* **2010**, *1* (21), 3207–3212.
- (19) Tang, Y.; Corbitt, T. S.; Parthasarathy, A.; Zhou, Z.; Schanze, K. S.; Whitten, D. G. *Langmuir* **2011**, *27* (8), 4956–4962.
- (20) Steen, H. B.; Boye, E.; Godal, T. *Cytometry* **1981**, *2* (2), 128–129.
- (21) Steen, H. B.; Boye, E.; Skarstad, K.; Bloom, B.; Godal, T.; Mustafa, S. *Cytometry* **1982**, *2* (4), 249–257.
- (22) Boye, E.; Steen, H. B.; Skarstad, K. *J. Gen. Microbiol.* **1983**, *129* (APR), 973–980.
- (23) Vandilla, M. A.; Langlois, R. G.; Pinkel, D.; Yajko, D.; Hadley, W. K. *Science* **1983**, *220* (4597), 620–622.
- (24) Berney, M.; Hammes, F.; Bosshard, F.; Weilenmann, H. U.; Egli, T. *Appl. Environ. Microbiol.* **2007**, *73* (10), 3283–3290.
- (25) Chen, P. S.; Li, C. S. *J. Environ. Monit.* **2005**, *7* (10), 950–959.
- (26) Berney, M.; Vital, M.; Hulshoff, I.; Weilenmann, H. U.; Egli, T.; Hammes, F. *Water Res.* **2008**, *42* (14), 4010–4018.
- (27) Lloyd, D.; Hayes, A. *J. FEMS Microbiol. Lett.* **1995**, *133* (1–2), 1–7.
- (28) Shapiro, H. M. *Practical Flow Cytometry*, 4th ed.; Wiley-Liss: Hoboken, NJ, 2003.
- (29) *Accuri\_Cytometers*, version 1.32, revision A, 2008.
- (30) Alvarez-Barrientos, A.; Arroyo, J.; Canton, R.; Nombela, C.; Sanchez-Perez, M. *Clin. Microbiol. Rev.* **2000**, *13* (2), 167–195.
- (31) Baena-Ruano, S.; Jimenez-Ot, C.; Santos-Duenas, I. M.; Cantero-Moreno, D.; Barja, F.; Garcia-Garcia, I. *Process Biochem.* **2006**, *41* (5), 1160–1164.
- (32) Bar, W.; Bade-Schumann, U.; Krebs, A.; Cromme, L. *J. Microbiol. Methods* **2009**, *77* (1), 85–89.
- (33) Saegeman, V. S. M.; De Vos, R.; Tebaldi, N. D.; van der Wolf, J. M.; Bergervoet, J. H. W.; Verhaegen, J.; Lismont, D.; Verduyck, B.; Ectors, N. L. *Microsc. Microanal.* **2007**, *13* (1), 18–29.
- (34) Shapiro, H. M. *Cytometry* **2001**, *43* (3), 223–226.
- (35) Alekshun, M. N.; Levy, S. B. *Cell* **2007**, *128* (6), 1037–1050.
- (36) Allegre, S.; Berger, F.; Berthelot, P.; Grattard, F.; Pozzetto, B.; Riffard, S. *Appl. Environ. Microbiol.* **2008**, *74* (24), 7813–7816.
- (37) Nikaido, H. *Microbiol. Mol. Biol. Rev.* **2003**, *67* (4), 593–656.
- (38) Mason, D. J.; Gant, V. A. *J. Antimicrob. Chemother.* **1995**, *36* (2), 441–443.
- (39) Mortimer, F. C.; Mason, D. J.; Gant, V. A. *Antimicrob. Agents Chemother.* **2000**, *44* (3), 676–681.
- (40) Wickens, H. J.; Pinney, R. J.; Mason, D. J.; Gant, V. A. *Antimicrob. Agents Chemother.* **2000**, *44* (3), 682–687.